WORLD CONFERENCE ON TIMBER ENGINEERING 2025
BRISBANE, AUSTRALIA
Advancing Timber for the Future Built Environment

COMPRESSIVE MECHANICAL PROPERTIES OF RADIATA PINE GRADED SAWN TIMBER CONSIDERING STRAIN RATE EFFECTS IN PROGRESSIVE COLLAPSE AND EARTHQUAKE EVENTS

Ayon Das[1], Nasim Ghasemi[2], Benoit P. Gilbert[3], Hong Guan[4], Chuen Yiu Lo[5], Minghao Li[6], Frank Lam[7]

ABSTRACT: The mechanical properties of timber are known to be sensitive to the rate at which loads are applied. Understanding these rate-dependent effects is crucial for the safe and robust design of timber structures, particularly in scenarios involving dynamic loading, such as earthquakes or progressive collapse events. This paper experimentally examines the influence of the strain rate on the compressive mechanical properties of free of knots specimens cut from Machine Graded Pine MGP10 radiata pine (*pinus radiata*) boards, considering strain rates representative of those experienced during progressive collapse and seismic events. Compression tests were performed both parallel and perpendicular-to-grain under four different loading rates, corresponding to nominal failure times of 0.2 s, 2 s, 20 s, and 200 s (quasi-static). A total of 160 tests were conducted following the method outlined in the European standard EN 408. For each test, the Modulus of Elasticity (MOE), compressive strength and ductility were measured. For the parallel-to-grain compression tests and the strain rates considered, the results showed that the average compressive strength increased by 16%, the MOE showed no statically significant difference, and the ductility decreased by 6%. For the perpendicular-to-grain tests, the average MOE and compressive strength increased by 32% and 53%, respectively. These findings highlight the rate-dependent behaviour of timber and emphasise the importance of considering strain rate effects in the structural design of timber components subjected to dynamic actions.

KEYWORDS: Radiata pine, Compressive strength, Strain rate effect, Modulus of elasticity, Ductility.

1 – INTRODUCTION

Timber has a long history as a construction material and continues to play a significant role in civil infrastructure. Traditional timber buildings remain prominent in many Asian countries such as in China, Japan and Korea [1, 2]. In recent decades, the development of Engineered Wood Products (EWPs) such as Cross-Laminated Timber (CLT), Glued Laminated Timber (Glulam) and Laminated Veneer Lumber (LVL) has significantly advanced the potential of timber construction. As a result, modern mass timber architecture, i.e., representing mid to high-rise buildings assembled from EWPs, is gaining worldwide traction. This global resurgence is exemplified by landmark projects such as Ascent (2022) [3] in the United States, the world's tallest hybrid timber buildings at 86.6 meters and Mjøstårnet (2019) [4] in Norway, a timber-only high-rise reaching 85.4 meters. Timber's growing appeal is also due to its low

[1] Ayon Das, School of Engineering and Built Environment, Griffith University, Gold Coast, Australia, ayon.das@griffithuni.edu.au

[2] Nasim Ghasemi, School of Engineering and Built Environment, Griffith University, Gold Coast, Australia, nasim.ghasemi@griffithuni.edu.au

[3] Benoit P. Gilbert, School of Engineering and Built Environment, Griffith University, Gold Coast, Australia, b.gilbert@griffith.edu.au

[4] Hong Guan, School of Engineering and Built Environment, Griffith University, Gold Coast, Australia, h.guan@griffith.edu.au

[5] Chuen Yiu Lo, School of Engineering and Built Environment, Griffith University, Gold Coast, Australia, c.lo@griffith.edu.au

[6] Minghao Li, Department of Wood Science, The University of British Columbia, Vancouver, Canada, minghao.li@ubc.ca

[7] Frank Lam, Department of Wood Science, The University of British Columbia, Vancouver, Canada, frank.lam@ubc.ca

https://doi.org/10.52202/080513-0125

environmental impact, natural aesthetics, superior thermal insulation, rapid assembly and high strength-to-weight ratio compared to traditional building materials like steel and concrete [5] .

Understanding the behaviour of Machine Graded Pine (MGP) [6] under different loading rates and directions is important for several reasons. Firstly, glulam is a key material used in mass timber construction due to its strength, versatility and sustainability [7]. In Australia, according to requirements in the standard AS 1328.1 [8], the timber used in the manufacturing of glulam shall be stress-graded. MGP-graded radiata pine (*pinus radiata*) and other softwood species sawn boards are commonly used in the manufacture of softwood glulam. Secondly, timber structures may be subjected to dynamic loading over their lifespan, such as earthquakes or progressive collapse events [9]. Thirdly, timber is an orthotropic material and its dynamic responses parallel and perpendicular-to-grain are different [9, 10]. As shown in Table 1, different loading types lead to different strain rate values which would affect the material's stiffness, strength and ductility differently [11, 12].

Table 1: Strain rate values under different loading types [10, 13]

Loading type	Strain rate (s^{-1})
Creep	10^{-8} to 10^{-6}
Quasi-static	10^{-6} to 10^{-2}
Earthquake	10^{-3} to 10^{-1}
Vehicle crash	10^{-1} to 10^{+1}
Blast / Impact / Explosion	1 to 10^{+6}

For mass timber buildings, the compressive strength of timber is a critical parameter in both member and connection design. Wood species and wood density are amongst the factors influencing this property [14]. Xie et al. [10] and Zhang et al. [9] demonstrated that the loading rate affects the Modulus of Elasticity (MOE) and strength, both in the parallel and perpendicular-to-grain directions. However, design rules in international standards are typically based on static tests and may not accurately consider the dynamic loading effects, particularly on properties beyond strength, such as the MOE and ductility. Such effects are typically accounted for by applying a load duration factor, which adjusts the quasi-static properties to estimate material behaviour under varying loading rates. For example, the Australian standard AS 1720.1 [6] and New Zealand standard NZS AS 1720.1 [15] use a load factor of 1.0 to calculate the strength of structural members with a 5 s load duration. The Eurocode 5 [14] applies a 1.10 load factor for instantaneous actions (wind or accidental), while the North American NDS [16] allows a 25% strength increase between quasi-static and impact loadings.

This study aims to improve the understanding of the influence of the strain rate on the mechanical behaviour of sawn timber by conducting compression tests, both parallel and perpendicular-to-grain, on knot-free samples cut from MGP10 graded timber [6]. Tests were carried out under varying strain rates, with failure times ranging from 0.2 seconds (representative of seismic and progressive collapse events) to 200 seconds (quasi-static conditions), following the procedures outlined in the European standard EN 408 [17]. The MOE, compressive strength and ductility were evaluated and are discussed in the paper.

2 – BACKGROUND

Published studies exploring the influence of dynamic strain rates on the mechanical properties of timber were mainly conducted by testing small clear samples and principally focussed on the compressive strength at high strain rates, corresponding to blast events [18, 19]. The study by Bragov and Lomunov [18] found that for strain rates ranging from 500 s^{-1} to 1,500 s^{-1}, the compressive strength of small pine, birch and lime specimens increased by up to 60% perpendicular and by 50-60% parallel-to-grain. Widehammar [19] observed that the dynamic compressive strength of spruce sapwood increased by 20% perpendicular and 50% parallel-to-grain between strain rates of 8×10^{-3} s^{-1} and 1,000 s^{-1}. Xie et al. [10] tested three softwood species, spruce, dahurian larch and Baltic pine under parallel-to-grain loading at strain rates ranging from 10^{-4} s^{-1} to 0.1 s^{-1}. Between the two strain rates, the compressive strength of the spruce, dahuran larch and Baltic pine increased by 16%, 23% and 14%, respectively. Zhang et al. [9] also observed similar trends on three wood species, consisting of dahurian larch, Mongolian pine and Chinese poplar, in the perpendicular-to-grain direction. All three species exhibited an increase in compressive strength with increasing strain rates. Between strain rate of 10^{-1} s^{-1} and 10^{-4} s^{-1} the compression strength increased by 15.9%, 16.9%, and 27.1% for the dahurian larch, Mongolian pine and Chinese poplar samples, respectively.

3 – MATERIALS AND METHODS

3.1 MATERIALS AND LOADING RATES

All specimens were prepared from MGP10 radiata pine softwood boards, commercially supplied by

NeXTimber® by Timberlink [20] and sourced from Victoria, Australia. The boards provided were 3,000 mm long, 45 mm thick and 90 mm wide. The samples were cut from 20 different boards according to the dimensions specified in the European standard EN 408 [17]. For each board and loading direction, four samples were cut, resulting in four sets of 20 nominally identical specimens. Since knots are known to influence the material properties of timber elements [21], to ensure consistency between strain rates, the samples were taken from board sections that allowed for knot-free specimens, with a knot-to-area ratio [22] less than 3% over the length. The parallel-to-grain specimens had nominal dimensions of 45 mm (thickness) × 90 mm (width) × 270 mm (length), while for the perpendicular-to-grain specimens, the length was reduced to 70 mm. The specimen geometries are shown in Figures 1 and 2 for the parallel and perpendicular-to-grain samples, respectively.

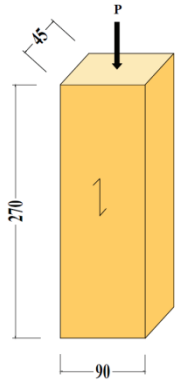

Figure 1. Compression test samples for parallel-to-grain showing the loading direction

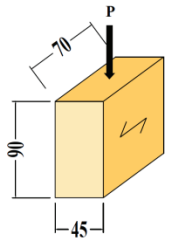

Figure 2. Compression test samples for perpendicular-to-grain showing the loading direction

For each loading direction, the four sets of nominally identical specimens were tested under four loading rates, targeting failure times of 200 s (quasi-static), 20 s, 2 s, and 0.2 s (representing seismic and progressive collapse scenarios). These times to failure correspond to strain rates in the order of 10^{-5} s^{-1} to 10^{-2} s^{-1}. The sample size of 20 specimens per strain rate was selected to ensure statistically meaningful results.

Before testing, all specimens were conditioned at 20°C in in an air-conditioned room. From each board, two moisture content samples (one sample for each loading direction) were cut and used to determine the moisture content at the time of testing using the oven-dry method in accordance to the Australian and New-Zealand standard AS/NZS 1080.1 [23]. The average moisture content was measured as 11.3% and 13.0%, with Coefficients Of Variation (COV) of 5% and 8%, for the parallel and perpendicular-to-grain samples, respectively. Additionally, the density of each sample was calculated from the measured mass and dimensions.

3.2 TEST METHODS

3.2.1 Parallel-to-grain test setup

The parallel-to-grain samples were tested in displacement control in a 500 kN MTS universal testing machine, as shown in Figure 3, following the procedure in the European standard EN 408 [17] with the modifications outlined below.

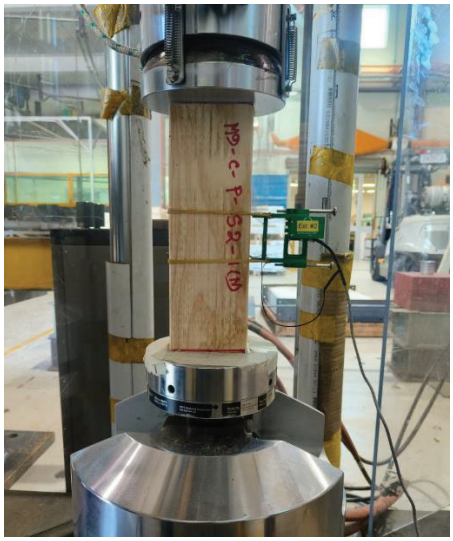

Figure 3. Setup for parallel-to-grain compression tests

Each sample was positioned at the centre of a fixed bottom platen. The load was applied through a top platen, mounted on a swivel so as to ensure uniform load distribution across the top surface. A 50 mm gauge-length (h_o) extensometer was attached at mid-height of the samples to measure the strain (ε) and calculate the

https://doi.org/10.52202/080513-0125

MOE parallel-to-grain (E_L). To normalise the initial loading condition, all specimens were quasi-statically preloaded to 1 kN and then unloaded to 0.5 kN, ensuring full contact with the loading surfaces before the final loading. The machine stroke (δ) was also recorded to assess the overall deformation and calculate the ductility of the different strain rates. Tests were stopped either when the displacement reached 4.5 mm or a 30% load drop was observed, which ever came first.

3.2.2 Perpendicular-to-grain test setup

The perpendicular-to-grain samples were tested in displacement control in 100 kN Instron universal testing machine, as shown in Figure 4, following a similar setup to the parallel-to-grain samples and the recommendations in the EN 408 [17]. While a 25 mm gauge-length extensometer was used to measure the strain deformation, due to a manipulation error, the strain data were incorrectly recorded and could not be used. The strain (ε) was then estimated using the stroke (δ) of the testing machine and the measured height of the samples. While it is understood that this method will not accurately measure the strain [24], it will still allow to compare the change (in percent) between the different strain rates of the MOE perpendicular-to-grain (E_{RT}). Preloading and loading were performed as for the parallel-to-grain samples. Tests were concluded either at a 6 mm displacement or when the load dropped by more than 30% of the maximum load.

Figure 4. Setup for perpendicular-to-grain compression tests

3.1.3 Parameters calculated

For each test, the compression stress (f) applied to the sample was determined as:

$$f = \frac{P}{A} \quad (1)$$

where P is the applied load and A is the measured cross-sectional area. The compression stress f - displacement δ curve was derived for each test to evaluate the following criteria illustrated in Figure 5:

- Time of failure, T_f: defined as the time at which the compressive strength is reached (see dot point below).
- Compression strength, f_c: defined as which ever came first between either the maximum stress at which a load drop occurred (Figure 5 (a)) or as the stress corresponding to the intersection of the stress-displacement curve with a line offset by $0.01h_t$ (where h_t is the height of the specimen along the loading direction) from the linear portion of the stress-displacement curve, determined using the iterative process described in EN 408 [17] (Figure 5 (b)).

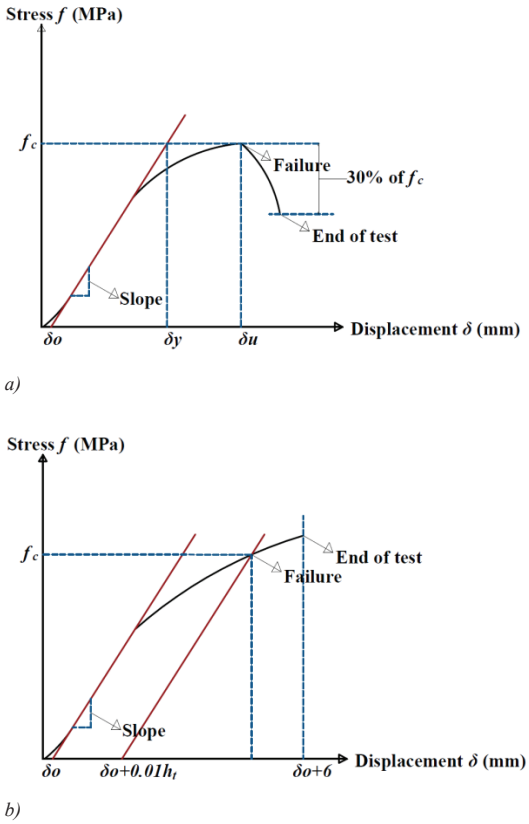

Figure 5. Evaluation criteria for compression strength, (a) in the case of load drop, and (b) in the case of no-load drop

- Ductility, Δ: evaluated only for the parallel-to-grain tests, as no load drop was typically observed in the perpendicular-to-grain direction, and determined as:

$$\Delta = \frac{\delta_u - \delta_0}{\delta_y - \delta_0} \quad (2)$$

where δ_u is the ultimate displacement taken at the compressive strength and δ_y is the yield displacement which is calculated as the displacement at the intersection of the linear slope of the stress-displacement curve (obtained by performing a linear regression between 10% and 40% of f_c) and the horizontal line at f_c, as shown in Figure 5 (a).

Additionally, the stress f - strain ε curves were used to determine the MOE, calculated as the slope of the linear portion of the curves, with the slope obtained by performing a linear regression between 10% and 40% of f_c. The characteristic compression strength value was also determined for each strain rate based on the number of tests conducted using the methodology outlined in Clause 3.2 of the European Standard EN 14358 (2016) [25] assuming lognormal distributions.

4 – RESULTS

4.1 COMPRESSION PARALLEL-TO-GRAIN

The compression stress–displacement curves for the samples tested parallel-to-grain under the four different strain rates are presented in Figure 6. The corresponding measured and calculated values, along with their COV, are summarised in Table 2.

The average compressive strength increased with increasing strain rate, showing a 16.4% increase from the lowest to the highest strain rate. The influence of strain rate observed in this study agrees from the findings of Xie et al. [10] who, using comparatively smaller samples but strain rates of the same order of magnitude, reported increases of 14–23%. However, the characteristic compressive strength only increased by 5% between the quasi-static and highest strain rates.

The strain rate showed no real influence on the average MOE, with the MOE slightly decreasing with increasing strain rate. Similarly, the ductility only decreased by 6% between the quasi-static and highest strain rates.

The influence of the strain rate found in the present work on the compression properties are further illustrated in the box-and-whisker plots in Figure 7. A linear relationship is typically observed between the reported properties and the logarithm of the failure time.

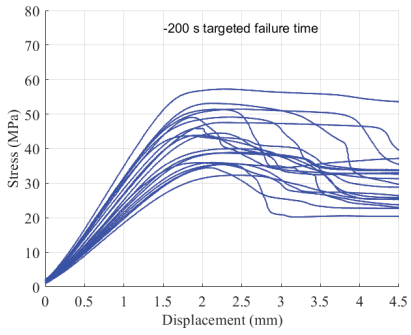

a)

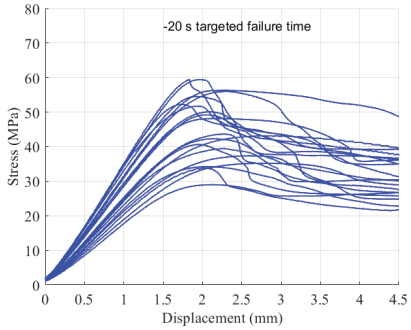

b)

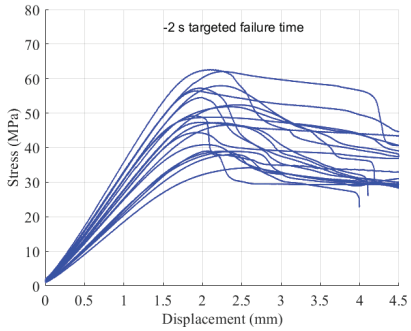

c)

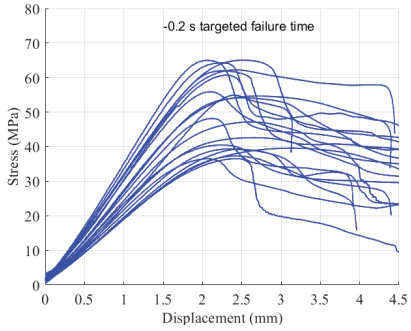

d)

Figure 6. Parallel-to-grain compression test stress-displacement curves for targeted failure in (a) 200 s, (b) 20 s, (c) 2 s, and (d) 0.2 s.

https://doi.org/10.52202/080513-0125

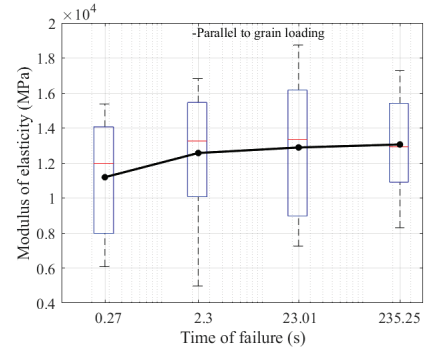

a)

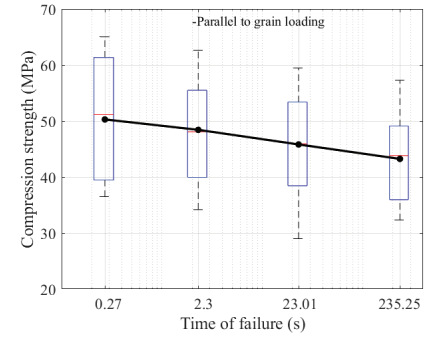

b)

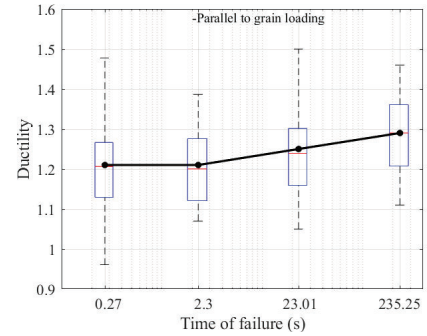

c)

Figure 7. Parallel-to-grain test results versus time of failure, (a) MOE, (b) compression strength and (c) ductility

Figure 8 shows the failure modes of two representative samples tested under quasi static loading conditions. No real differences were observed between the failure modes across the different strain rate groups.

a)

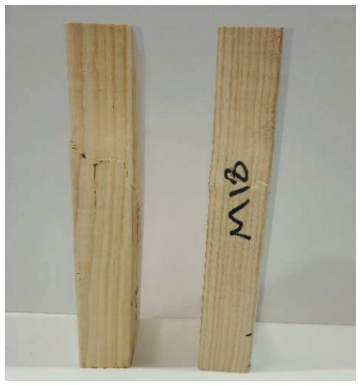

b)

Figure 8. Failure modes of representative samples tested parallel-to-grain (a) front view, and (b) side view

4.2 COMPRESSION PERPENDICULAR-TO-GRAIN

The compression stress-displacement curves for the perpendicular-to-grain embedment tests are presented in Figure 9 for the four different strain rates. The measured and calculated values are detailed in Table 3.

Table 2. Compression parallel-to-grain test results

Number of tests	*Density*		T_f		E_L		f_c			Δ	
	Average (kg/m³)	*COV (%)*	*Average (s)*	*COV (%)*	*Average (MPa)*	*COV (%)*	*Average (MPa)*	*COV (%)*	*Charac-teristic (MPa)*	*Average*	*COV (%)*
20	507	10.8	235	8.8	13,058	21.6	43.2	16.8	30.9	1.29	7.7
20	511	10.7	23	12.8	12,886	29.4	45.8	20.1	30.1	1.25	9.9
20	513	10.3	2.3	8.5	12,570	26.1	48.4	17.4	34.0	1.21	7.8
20	510	10.4	0.3	12.6	11,188	28.4	50.3	21.3	32.5	1.21	9.7

https://doi.org/10.52202/080513-0125

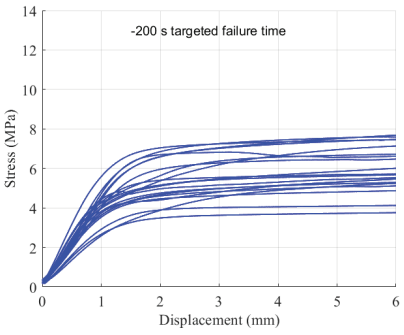

a)

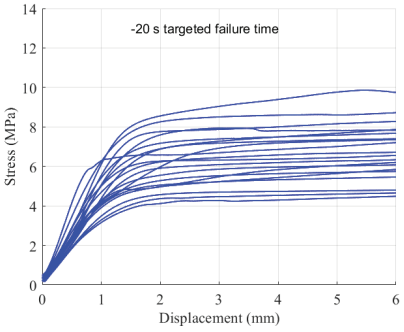

b)

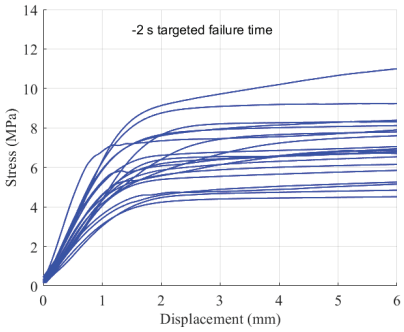

c)

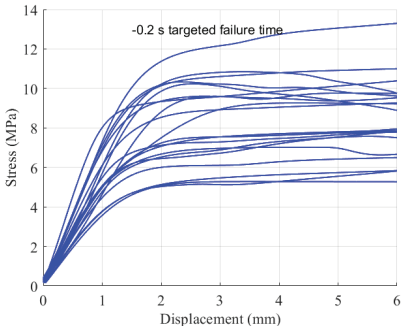

d)

Figure 9. Perpendicular-to-grain compression test stress-displacement curves for targeted failure in (a) 200 s, (b) 20 s, (c) 2 s, and (d) 0.2 s.

The strain rate also affected the compression properties perpendicular-to-grain, with both the MOE and the compressive strength rising as the strain rate increased. Comparing failures between 200 s and 0.2 s, the MOE increased by 31.9% and the compression strength by 52.8% which are notably higher than the changes observed in the parallel-to-grain direction. These increases are greater than the results reported by Zhang et al. [9] for similar strain rates. The characteristic compressive strength increased by 38.2% from the quasi-static to the highest strain-rate conditions.

The results are further illustrated in the box-and-whisker plots in Figure 10. The figure shows a nearly linear relationship between the average MOE and compression strength, and the logarithm value of the failure time.

Figure 11 illustrates the failure modes of one representative specimen tested under high loading rates. Under all strain rates, the samples exhibited buckling and yielding.

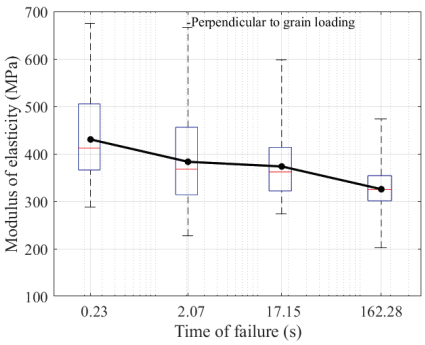

a)

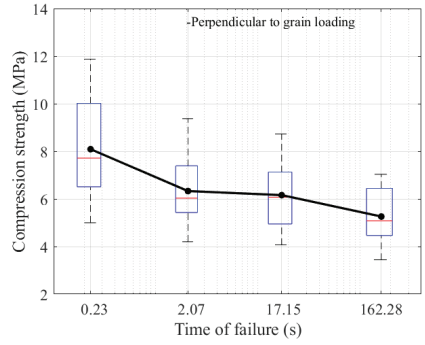

b)

Figure 10. Perpendicular-to-grain test results versus time of failure, (a) modulus of elasticity and (b) compression strength

https://doi.org/10.52202/080513-0125

Table 2. Compression perpendicular-to-grain test results

Number of tests	Density		T_f		E_{RT}[1]		f_c			Δ	
	Average (kg/m³)	COV (%)	Average (s)	COV (%)	Average (MPa)	COV (%)	Average (MPa)	COV (%)	Charac-teristic (MPa)	Average	COV (%)
20	530	10.8	162	13.9	326	19.2	5.3	21.3	3.4	N/A	
20	520	10.9	17	15.3	373	21.3	6.2	22.3	3.9	N/A	
20	510	11.9	2.1	12.8	383	26.6	6.3	23.0	4.0	N/A	
20	520	12.8	0.23	37.3	430	22.8	8.1	25.8	4.7	N/A	

(1) Values calculated using the stroke of the testing machine to obtain the strain and not representative of the actual MOE values

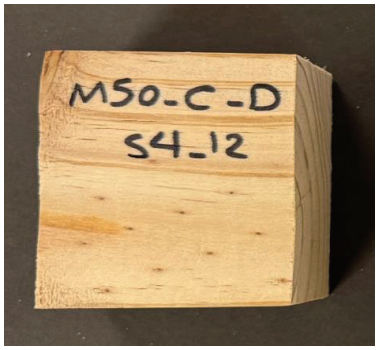

a)

b)

Figure 11. Failure mode of representative samples tested perpendicular-to-grain (a) front view, and (b) side view

5 – CONCLUSION

In this work, the impact of strain rate on the compressive performance of knot-free specimens cut from MGP10 graded timber was assessed for failure times ranging from 200 s (quasi-static) to 0.2 s (seismic and progressive-collapse loading). The experiments demonstrated that the strain rate affects the material's compression properties. Across the tested strain rate range, the following key observations were made:

- The MOE showed not to be significantly influenced by the strain rate in the parallel-to-grain direction, however, in the perpendicular-to-grain direction, it increased by 31.9% between failure times of 200 s and 0.2s.
- The compression strength increased by 16.4% (parallel) and 52.8% (perpendicular) over the same failure time range while the characteristic strength rose by 5.0% (parallel) and 38.0% (perpendicular).
- When loaded parallel-to-grain, the ductility decreased by 6% as failure time decreased from 200 s to 0.2 s. The failure mode remained ductile throughout all perpendicular-to-grain tests.

These observations indicate that the strain rate critically influences both the MOE and compressive strength of sawn timber, with a higher influence when loading perpendicular-to-grain. The consequences on the seismic and progressive collapse design of timber structures, as well as associated connections, needs to be further analysed.

6 - ACKNOWLEDGEMENTS

This project is funded by the Australian Research Council under Discovery Project DP230100460. The authors would like to thank NeXTimber® by Timberlink for providing the MGP10 materials.

7 – REFERENCES

[1] Fang, D., et al., Ancient Chinese timber architecture. I: Experimental study. Journal of structural engineering, 2001. 127(11): p. 1348-1357.

[2] Oudjene, M. and M. Khelifa, Elasto-plastic constitutive law for wood behaviour under compressive loadings. Construction and Building Materials, 2009. 23(11): p. 3359-3366.

[3] Fernandez, A., J. Komp, and J. Peronto, Ascent-challenges and advances of tall mass timber construction. International Journal of High-Rise Buildings, 2020. 9(3): p. 235-244.

[4] Abrahamsen, R. Mjøstårnet-Construction of an 81 m tall timber building. in Internationales Holzbau-Forum IHF. 2017.

[5] Roos, A., L. Woxblom, and D. McCluskey, The influence of architects and structural engineers on timber in construction–perceptions and roles. Silva Fennica, 2010. 44(5): p. 871-884.

[6] AS1720.1: Timber structures Part 1: Design Methods. Australian Standards, 2010.

[7] Abed, J., et al., A Review of the Performance and Benefits of Mass Timber as an Alternative to Concrete and Steel for Improving the Sustainability of Structures. Sustainability, 2022. 14(9).

[8] AS NZS 1328.1: Glued laminated structural timber, part 1: Performance requirements and minimum production requirements. Australian and New Zealand Standard, 1998.

[9] Zhang, L., et al., Effects of seismic strain rates on the perpendicular-to-grain compression behaviour of Dahurian larch, Mongolian pine and Chinese poplar: tests and stress-strain model. Holzforschung, 2023. 77(6): p. 383-393.

[10] Xie, Q., et al., Dynamic parallel-to-grain compressive properties of three softwoods under seismic strain rates: tests and constitutive modeling. Holzforschung, 2020. 74(10): p. 927-937.

[11] Cheng, X., et al., Strain Rate Effect on the Embedment Mechanical Properties and Fracture Behavior of Softwood Laminated Veneer Lumbers: Implications to Timber Connections. Journal of Structural Engineering, 2023. 149(9).

[12] Wood, L.W., Relation of strength of wood to duration of load. 1951: US Department of Agriculture, Forest Service, Forest Products Laboratory.

[13] Velmurugan, R., D. Ruan, and S. Gurusideswar, Composite Materials: High Strain Rate Studies. 2023.

[14] EN 1995-1-1,Eurocode 5: Design of timber structures—Part 1-1: General—Common rules and rules for buildings. European Committee for Standardization, Brussel, Belgium: CEN., 2004.

[15] NZS AS 1720.1: Timber structures Part 1: Design methods. New Zealand Standard, 2022.

[16] NDS: National Design Specification for Wood Construction American Wood Council (AWC) and ANSI (American National Standards Institute), 2024.

[17] EN 408, Timber structures — Structural timber and glued laminated timber — Determination of some physical and mechanical properties. EN 408. London, UK: British Standards Institution. 2010.

[18] Bragov, A. and A.K. Lomunov, Dynamic properties of Some Wood Species. Le Journal de Physique IV, 1997. 07(C3): p. C3-487-C3-492.

[19] Widehammar, S., Stress-Strain Relationships for Spruce Wood: Influence of Strain Rate, Moisture Content and Loading Direction. Experimental Mechanics, 2004. 44(1): p. 44-48.

[20] Timberlink, Australian-made engineered wood products and mass timber building solutions. www.timberlinkaustralia.com.au, Accessed on: 14/05/2025.

[21] Ashby, M.F. and L.J. Gibson, Cellular solids: structure and properties. Press Syndicate of the University of Cambridge, Cambridge, UK, 1997: p. 175-231.

[22] Fink, G. and J. Kohler, Model for the prediction of the tensile strength and tensile stiffness of knot clusters within structural timber. European Journal of Wood and Wood Products, 2014. 72: p. 331-341.

[23] AS/NZS 1080.1:Timber—Methods of test—Moisture content. Sydney, NSW, Australia: AS. Australian Standards, 2012.

[24] Gilbert, B.P., D. Fernando, and C.H. Pham, Experimental techniques in structural Testing: Common Mistakes, how to avoid them and other advice. Structures, 2022. 41: p. 1687-1699.

[25] EN 14358: Timber structures— Calculation and verification of characteristic values. Brussel, Belgium: CEN. European Committee for Standardization, 2016.

https://doi.org/10.52202/080513-0125